

# Quantum Logic with a Few Trapped Ions

C. Monroe, W. M. Itano, D. Kielpinski, B. E. King, D. Leibfried,  
C. J. Myatt, Q. A. Turchette, D. J. Wineland, and C. S. Wood

*Time and Frequency Division,  
National Institute of Standards and Technology  
Boulder, CO 80303*

**Abstract.** Small laser-cooled crystals of atomic ions have attracted considerable interest in the last several years for their possible application toward quantum computation. This paper considers quantum logic schemes for small numbers of ions in the context of recent experiments at NIST.

## I INTRODUCTION

In its simplest form, a quantum computer is a collection of  $N$  two-level quantum systems (quantum bits) which can be prepared in an arbitrary entangled quantum state spanning all  $2^N$  basis states [1,2]. A quantum computer, unlike its classical counterpart, can thus store and simultaneously process superpositions of numbers. Once a measurement is performed on the quantum computer, the superposition collapses to a single number, which in some cases can jointly depend on all of the numbers previously stored. This gives the potential for massive parallelism in particular algorithms [3], most notably an efficient factoring algorithm [2,4] and a fast searching algorithm [5]. Apart from these and other possible applications [6], creating multi-particle entangled states is of great interest in its own right, from the standpoint of quantum measurement theory [7], and for improved signal-to-noise ratio in spectroscopy [8,9].

Unfortunately, very few physical systems are amenable to the task of quantum computation. This is because the quantum bits must (i) interact very weakly with the environment to preserve coherence of their superpositions, and (ii) interact very strongly with other quantum bits to facilitate the construction of quantum logic gates necessary for computing. In addition to these seemingly conflicting requirements, the quantum bits must be able to be controlled and manipulated coherently and be read out with high efficiency.

In 1995, Cirac and Zoller showed that a collection of trapped and cooled atomic ions can satisfy these requirements and form an attractive quantum computer architecture [10]. In their proposal, each quantum bit is derived from a pair of internal energy levels of an individual atomic ion. The quantum bits are coupled to one another by virtue of the quantized collective motion of the ions in the trap, mediated by the Coulomb interaction. Cirac and Zoller showed that an arbitrary entangled state can be created and permit any quantum computation by applying several laser pulses, each interacting with a single ion at a time. In light of recent experiments at NIST with two ions [11,12], this paper considers alternative quantum logic schemes, where laser pulses simultaneously interact with a few ions and their collective motional modes to produce entangled states.

## II BACKGROUND

### A Internal Electronic States of Ions as Quantum Bits

Ions can be confined for days in an ultra-high vacuum with minimal perturbations to their internal atomic structure, making particular internal states ideal for representing a quantum bit. Even though the ions interact strongly through their mutual Coulomb interaction, the fact that the ions are localized means that the time-averaged value of the electric field they experience vanishes; therefore electric field perturbations are small.

*CP457, Trapped Charged Particles and Fundamental Physics*  
edited by Daniel H. E. Dubin and Dieter Schneider  
1999 The American Institute of Physics 1-56396-776-6/99/\$15.00

Although magnetic field perturbations to internal structure are important, the coherence time for superposition states of two internal levels can be made very long by operating at fields where the energy separation between levels is at an extremum with respect to field. For example, a coherence time exceeding 10 minutes between a pair of  ${}^9\text{Be}^+$  ground state hyperfine levels has been observed [13]. It is also possible to employ a ground and excited (metastable) electronic state of a trapped ion as a quantum bit. This option seems difficult at present, because the energy splittings are typically in the optical region and thus an extremely high laser frequency stability is required to drive coherent transitions.

Figure 1(a) shows a reduced energy level diagram of a single  ${}^9\text{Be}^+$  ion. Although many other ion species would also be suitable for quantum computation, we will concentrate on  ${}^9\text{Be}^+$  here for concreteness and to make a connection to the experiments at NIST [11,12,14,15]. We will be interested primarily in two electronic states, the  ${}^2S_{1/2}(F = 2, m_F = 2)$  and  ${}^2S_{1/2}(F = 1, m_F = 1)$  hyperfine ground states (denoted by  $|\downarrow\rangle$  and  $|\uparrow\rangle$  respectively), separated in energy by  $\hbar\omega_0$ . These long-lived spin states will form the basis for a quantum bit. Standard optical pumping techniques allow the spin to be initialized into either  $|\downarrow\rangle$  or  $|\uparrow\rangle$ . Subsequent detection of the spin states can be accomplished using the technique of quantum jumps [16]. By tuning a circularly polarized laser beam to the  ${}^2P_{3/2}$  transition at  $\lambda_{Be} = 313$  nm (Fig. 1(a)), many photons are scattered if the atom is in the  $|\downarrow\rangle$  spin state (a “cycling” transition), but essentially no photons are scattered if the atom is in the  $|\uparrow\rangle$  spin state. If a modest number of these photons are detected, the efficiency of our ability to discriminate between these two states approaches 100%.

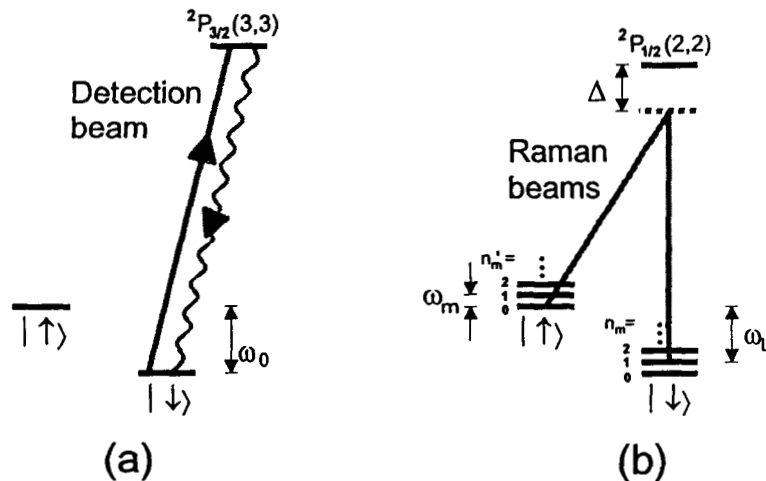


**FIGURE 1.** (a) Electronic (internal) energy levels (not to scale) of a  ${}^9\text{Be}^+$  ion. The  ${}^2S_{1/2}(F = 2, m_F = 2)$  and  ${}^2S_{1/2}(F = 1, m_F = 1)$  hyperfine ground states (denoted by  $|\downarrow\rangle$  and  $|\uparrow\rangle$  respectively), separated in frequency by  $\omega_0/2\pi \simeq 1.250$  GHz, form the basis of a quantum bit. Detection of the internal state is accomplished by illuminating the ion with a  $\sigma^+$ -polarized “detection” beam near  $\lambda_{Be} \simeq 313$  nm, which drives the cycling  $|\downarrow\rangle \rightarrow {}^2P_{3/2}(F = 3, m_F = 3)$  transition, and observing the scattered fluorescence. The excited P state has radiative linewidth  $\gamma/2\pi \simeq 19.4$  MHz. (b) Energy levels of a trapped  ${}^9\text{Be}^+$  ion, including the motional states of a single mode  $m$  of harmonic motion, depicted by ladders of vibrational states separated in frequency by the mode frequency  $\omega_m$ . Two Raman beams, both detuned by  $\Delta \gg \omega_0, \omega_m$  from the excited  ${}^2P_{1/2}$  state, provide a coherent two-photon coupling between states  $|\downarrow\rangle|n_m\rangle$  and  $|\uparrow\rangle|n'_m\rangle$  by setting the difference frequency  $\omega_L$  to match the desired transition frequency. As shown, the Raman beams are tuned to the first red sideband of mode  $m$  ( $\omega_L = \omega_0 - \omega_m$ ).

## B Collective Motional States of a Linear Crystal

Ions can be confined in several types of electromagnetic traps. Here, we consider the rf (Paul) ion trap, in which an oscillating electric potential is applied to electrodes surrounding the ions. In the standard quadrupole-like rf trap, the potential varies in space and time as

$$\Phi \simeq [U_0 + V_0 \cos(\Omega_T t)] \left( \frac{\alpha x^2 + (1 - \alpha)y^2 - z^2}{d_T^2} \right), \quad (1)$$

where  $d_T$  characterizes the trap electrode dimension and  $0 < \alpha \leq 1/2$  characterizes the geometrical anisotropy of the trap electrodes ( $\alpha = 1/2$  corresponds to a quadrupolar potential). This gives rise to harmonic ponderomotive potentials [17] in all three dimensions with oscillation frequencies

$$\omega_x = \frac{\Omega_T}{2} \sqrt{\alpha a + \frac{\alpha^2 q^2}{2}} \quad (2a)$$

$$\omega_y = \frac{\Omega_T}{2} \sqrt{(1-\alpha)a + \frac{(1-\alpha)^2 q^2}{2}} \quad (2b)$$

$$\omega_z = \frac{\Omega_T}{2} \sqrt{-a + \frac{q^2}{2}}, \quad (2c)$$

where  $a = 8eU_0/(m\Omega_T^2 d_T^2)$  and  $q = 4eV_0/(m\Omega_T^2 d_T^2)$  and  $e/M$  is the charge-to-mass ratio of the ion. In these expressions, it is assumed that  $-\alpha q^2/2 < a < q^2/2$  and  $q \ll 1$  (or equivalently  $\omega_{x,y,z} \ll \Omega_T$ )—a condition known as the “pseudopotential approximation” [17]. Motion described by an rf pseudopotential is always accompanied by micromotion at frequencies near  $\Omega_T$  associated with the rf electric fields. An alternative geometry is the linear trap [18], in which a 2D pseudopotential confines ions radially and an independently applied static potential confines the ions axially. Because the rf fields vanish along the axial node, there is no axial micromotion, and many of the problems associated with micromotion are avoided. For this reason, the linear rf trap is more appropriate when larger numbers of ions are confined and micromotion is not desired.

For a collection of trapped ions, the mutual Coulomb repulsion counteracts the confining potential, and if the ions are sufficiently cold, they will crystallize to an equilibrium configuration. In this case, the three frequencies in Eq. (2) describe center-of-mass (COM) harmonic motion, and a normal mode calculation must be done to solve for the other internal modes of harmonic motion. The simplest crystalline structure is a linear chain, which can be attained with a sufficiently anisotropic trap. Here, we will take the  $x$ -axis in the above expressions to represent the weakest (axial) direction of the trap, which can be ensured by setting  $a < 0$  and  $\alpha < 1/2$ . For  $N = 2$  ions, the ions will clearly arrange themselves along the  $x$ -axis of the trap. For  $N=3$  ions, the ions will form a linear chain along  $x$  only if  $\omega_x < \sqrt{5/12} \omega_{y,z}$ . For larger numbers of ions, this anisotropy must be even larger, and has been numerically calculated in Ref [19].

Of the  $3N$  normal modes of small oscillation in a linear chain of ions, we are primarily interested in the  $N$  collective modes associated with axial motion (assumed to be along the  $x$ -direction in the above equations). A remarkable feature of a linear chain of ions is that the axial mode frequencies are nearly independent of

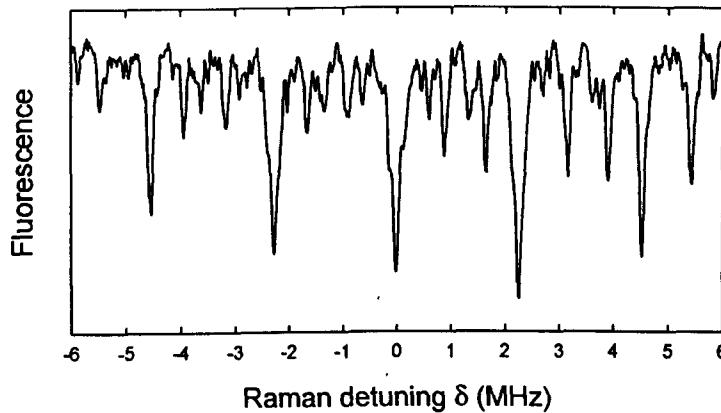


**FIGURE 2.** Raman absorption spectrum of three trapped ions. The ordinate is the detuning  $\delta$  of the Raman probe beam difference frequency and the abscissa shows the ion fluorescence, proportional to the number of ions in the state  $|\downarrow\rangle$  (the ions are initially prepared in state  $|\downarrow\rangle|\downarrow\rangle|\downarrow\rangle$ ). The carrier appears at  $\delta = 0$ , and the first sidebands of the three axial normal modes of motion appear at  $\delta = \pm 2.25, \pm 3.90$ , and  $\pm 5.43$  MHz, in agreement with the theoretical frequency ratios  $1 : \sqrt{3} : \sqrt{29/5}$ . Several higher order sidebands also appear at sums and differences of harmonics of the normal mode frequencies.

$N$  [10,20,21], offering the possibility that mode interference might be small, even for large numbers of ions. For two ions, the axial normal mode frequencies are  $\omega_x$  and  $\sqrt{3}\omega_x$ ; for three ions they are  $\omega_x, \sqrt{3}\omega_x$ , and  $\sqrt{29/5}\omega_x$ , as shown in Fig. 2. For  $N > 3$  ions, the normal modes must be determined numerically [20,21]. The quantum state of a particular axial mode  $m$  of motion at frequency  $\omega_m$  is represented by the ladder of vibrational eigenstates  $|n_m\rangle$  of energy  $\hbar\omega_m(n_m + 1/2)$  with vibrational index  $n_m$  describing the number of phonons contained in the  $m$ th collective mode of motion. The motional modes can be initialized to the  $n_m = 0$  ground state through laser-cooling [11,14]. Whenever possible, operations involving the COM modes should be avoided, as the COM modes are found to lose coherence (through external heating) at an anomalously high rate [14,22] compared to the non-COM modes [11].

### C Interaction between Internal and Motional States

We now describe the coupling between the internal electronic levels and the collective axial motion of the ions when a classical radiation field is applied. If the internal levels  $|\downarrow\rangle_i$  and  $|\uparrow\rangle_i$  of the  $i$ th ion in a string are coupled by a dipole moment operator  $\mu_i$  (other couplings can be shown to behave analogously), then exposing the ions to traveling-wave electric fields  $\mathbf{E}_i(\mathbf{r}) = \tilde{\mathbf{E}}_i \cos(\mathbf{k} \cdot \mathbf{r} - \omega_L t + \phi_L)$  with frequency  $\omega_L$ , phase  $\phi_L$ , and wavevector  $\mathbf{k}$  results in the interaction Hamiltonian [22]

$$\mathcal{H} = \sum_{i=1}^N -\mu_i \cdot \mathbf{E}_i(\mathbf{r}_i) = \hbar \sum_{i=1}^N g_i \left( S_+^i e^{i(k_x \hat{X}_i - \delta t + \phi_L)} + S_-^i e^{-i(k_x \hat{X}_i - \delta t + \phi_L)} \right) \quad (3)$$

under the rotating wave approximation ( $|\delta|, g \ll \omega_0$ ). In this expression,  $g_i = -\langle \uparrow | \mu_i | \downarrow \rangle \cdot \tilde{\mathbf{E}}_i / 4\hbar$  is the resonant Rabi frequency connecting  $|\downarrow\rangle_i$  to  $|\uparrow\rangle_i$  in the absence of confinement,  $S_{\pm}^i$  are the internal level raising and lowering operators for the  $i$ th ion,  $\delta = \omega_L - \omega_0$  is the detuning of the radiation from atomic resonance, and  $k_x$  and  $\hat{X}_i = \mathbf{r}_i \cdot \hat{\mathbf{x}}$  are the axial components of the wavevector and position operator of the  $i$ th ion, respectively.

In practice, driving direct transitions between  $|n_m\rangle | \downarrow \rangle_i$  and  $|n'_m\rangle | \uparrow \rangle_i$  with rf or microwave radiation is not feasible, because the coupling between internal and motional states is proportional to powers of  $k_x$  from Eq. (3) and would thus be extremely small due to the long wavelength of the radiation. Alternatively, optical fields can be used to drive two-photon stimulated Raman transitions [14]. As depicted in Fig. 1(b), two laser beams detuned by  $\Delta$  from an excited state of radiative width  $\gamma$  are applied to the  $j$ th ion with their difference frequency matched to the desired transition frequency. For sufficient detuning  $|\Delta| \gg \gamma$ , the excited state may be adiabatically eliminated, and the above coupling of Eq. (3) applies, with  $g_i$  replaced by  $g_{i1}g_{i2}/\Delta$ , where  $g_{i1}$  and  $g_{i2}$  are the individual Rabi frequencies of the two beams when resonantly coupled to the excited level of ion  $i$ . In addition,  $\omega_L$  ( $\phi_L$ ) is replaced by the difference frequency (phase) of the beams, and  $\mathbf{k}$  is replaced by the difference in wavevectors of the two Raman beams  $\mathbf{k}_1 - \mathbf{k}_2$ . Since the relevant frequency depends only on the microwave difference between the two laser frequencies, both beams can be generated with a single laser source and a modulator, thereby relaxing the constraints of laser frequency stabilization.

Each ion in a linear array will be displaced from the axial center of the trap due to the other ions by an amount  $\bar{X}_i = eF_i/M\omega_x^2$ , where  $F_i$  is the static axial electric field at the  $i$ th ion due to the distribution of charges of the other ions in addition to any externally applied uniform axial field. (The force  $eF_i$  is of course balanced by the confining force of the trap.) If the ions are not confined in a linear trap, this displacement will cause each ion to undergo micromotion at the rf drive frequency  $\Omega_T$ . In the pseudopotential approximation, the axial position operator of the  $i$ th ion takes the form [17]

$$\hat{X}_i = \bar{X}_i + \hat{x}_i + \xi_i \cos(\Omega_T t). \quad (4)$$

In Eq. (4), the position of ion  $i$  is broken into three parts: a static offset term  $\bar{X}_i$  which can be combined with  $\phi_L$  in Eq. (3) to give an overall phase  $\phi_i = \phi_L + k_x \bar{X}_i$  at ion  $i$ , a quantum operator  $\hat{x}_i$  associated with small harmonic oscillations about the ion's equilibrium position at the normal mode frequencies, and a classical micromotion oscillation at  $\Omega_T$  with amplitude  $\xi_i = \bar{X}_i \alpha q / 2 = e\alpha q F_i / 2M\omega_x^2$ . A classical treatment of the micromotion is justified because even for unreasonably small fields  $F_i$ , the classical amplitude of micromotion is much greater than the zero-point motion ( $\xi_i \gg \sqrt{\hbar/M\omega_x}$ ). The quantum effects of micromotion typically amount to small corrections to the the treatment here [23].

The quantum portion  $\hat{x}_i$  of the position can be expressed in terms of the  $N$  axial harmonic oscillator normal mode raising and lowering operators  $\hat{a}_k^\dagger$  and  $\hat{a}_k$ :

$$\hat{x}_i = \sum_{k=1}^N D_k^i q_{k,0} (\hat{a}_k e^{-i\omega_k t} + \hat{a}_k^\dagger e^{i\omega_k t}). \quad (5)$$

In this expression,  $D_k^i$  is the normal mode transformation matrix which relates the  $i$ th ion's physical coordinate to the  $k$ th collective normal mode coordinate with zero-point characteristic size  $q_{k,0} = \sqrt{\hbar/2M\omega_k}$ .

When Eqs. (4) and (5) are substituted into the interaction Hamiltonian of Eq. (3), resonances (time independent interaction terms) occur when the detuning is set to sums of harmonics of all normal mode frequencies  $\omega_k$  and rf drive frequency  $\Omega_T$

$$\delta = \sum_{k=1}^N (n'_k - n_k)\omega_k + \ell\Omega_T, \quad (6)$$

where  $n'_k$ ,  $n_k$ , and  $\ell$  are integers. The resulting Hamiltonian matrix element which couples the quantum states  $|\downarrow\rangle_i|\{n\}\rangle$  and  $|\uparrow\rangle_i|\{n'\}\rangle$  ( $\{n\} = n_1, \dots, n_N$  and  $\{n'\} = n'_1, \dots, n'_N$ ) is

$$\mathcal{H}'' = \hbar \sum_{i=1}^N g_i e^{i\ell\pi/2} J_\ell(k_x \xi_i) \left( S_+^i e^{i\phi_i} \prod_{k=1}^N e^{i\eta_{i,k}(\hat{a}_k + \hat{a}_k^\dagger)} + h.c. \right), \quad (7)$$

where  $\eta_{i,k} = k_x D_k^i q_{k,0}$  is the Lamb-Dicke parameter of the  $i$ th ion associated with the  $k$ th normal mode, and  $J_\ell(z)$  is the  $\ell$ th Bessel function.

Typically, not all of the motional modes are altered upon application of this interaction, and we will treat two special cases:

(i) **Carrier Interaction.** When the radiation is tuned to the carrier, defined by  $\{n'\} = \{n\}$  in Eq. (6), no motional states are altered and there is no entanglement between internal and motional states. Each ion independently evolves between states  $|\downarrow\rangle_i|\{n\}\rangle$  and  $|\uparrow\rangle_i|\{n\}\rangle$  with coupling

$$\mathcal{H}_{c_i}'' = \hbar g_i e^{i\ell\pi/2} J_\ell(k_x \xi_i) \left( \prod_{k=1}^N \mathcal{R}_{i,k}(n_k) \right) (S_+^i e^{i\phi_i} + h.c.). \quad (8)$$

(ii) **Single-mode Interaction.** Here, the radiation is tuned to  $\delta = (n'_m - n_m)\omega_m + \ell\Omega_T$  so that only mode  $m$  is altered. This interaction is also called the " $n'_m - n_m$  motional sideband" on mode  $m$  and takes the form

$$\mathcal{H}_1'' = \hbar \sum_{i=1}^N g_i e^{i\ell\pi/2} J_\ell(k_x \xi_i) \left( \prod_{\substack{k=1 \\ (k \neq m)}}^N \mathcal{R}_{i,k}(n_k) \right) \left( S_+^i e^{i\eta_{i,m}(\hat{a}_m + \hat{a}_m^\dagger) + i\phi_i} + h.c. \right). \quad (9)$$

More-complicated multimode expressions can be similarly derived, allowing the engineering of a large class of interactions by simply tuning the radiation [22].

The factors which appear in Eqs. (8) and (9) are

$$\mathcal{R}_{i,k}(n_k) = \langle n_k | e^{i\eta_{i,k}(\hat{a}_k + \hat{a}_k^\dagger)} | n_k \rangle = e^{-\eta_{i,k}^2/2} \mathcal{L}_{n_k}(\eta_{i,k}^2), \quad (10)$$

describing the effect of motion in spectator motional mode  $k$  containing  $n_k$  quanta [22], where  $\mathcal{L}_n(z)$  is the  $n$ th Laguerre polynomial. Both  $\mathcal{R}_{i,k}(n_k)$  and  $J_\ell(k_x \xi_i)$  factors are  $\leq 1$  and can be interpreted as a suppression in the laser-ion interaction from the smearing-out of the ion's wavefunction due to spectator normal mode motion and micromotion, respectively. (These factors are known as Debye-Waller factors in many condensed-matter systems [24].)

The central ingredient in the single-mode coupling  $\mathcal{H}_1''$  is the coupling of the  $i$ th ion's internal states (operated by  $S_\pm^i$ ) to the  $m$ th normal mode (operated by  $\hat{a}_m$  and  $\hat{a}_m^\dagger$ ) which can allow entangled states to be created. In general, this interaction couples all  $2^N$  internal levels of the  $N$  ions in addition to many energy levels of the  $m$ th mode of motion. The Schrödinger equation must therefore be intergrated numerically to evaluate the amplitudes of all these energy levels. However, there are special cases which significantly simplify this coupling and can be used for quantum logic.

## 1 Individual Addressing of Ions by Focussing

In the Cirac-Zoller scheme for quantum logic, the interaction of Eq. (7) is sequentially applied to different ions in the string by focussing laser radiation on the individual ions. For example, if ion  $j$  is selected,  $g_i = \delta_{i,j}g$  and the sum in Eq. (7) collapses to a single term, resulting in a coupling between the two quantum states  $|\downarrow\rangle_j|\{n\}\rangle$  and  $|\uparrow\rangle_j|\{n'\}\rangle$  with matrix element

$$\langle\{n'\}|\downarrow\rangle_j|\mathcal{H}''|\downarrow\rangle_j|\{n\}\rangle = \hbar g_j e^{i\ell\pi/2} J_\ell(k_x \xi_j) e^{i\phi_j} \prod_{k=1}^N e^{-\eta_{j,k}^2/2} \eta_{j,k}^{|n'_k - n_k|} \sqrt{\frac{n_{k<}!}{n_{k>}!}} L_{n_{k<}}^{|n'_k - n_k|}(\eta_{j,k}^2), \quad (11)$$

where  $n_{k>} (n_{k<})$  is the greater (lesser) of  $n'_k$  and  $n_k$ , and  $L_n^\alpha(z)$  is a generalized Laguerre polynomial.

We will be interested primarily in three types of transitions on ion  $j$  involving one mode  $m$  of motion, selected by the detuning  $\delta$ : the carrier, the  $-1$  or "first red" sideband of mode  $m$ , and the  $+1$  or "first blue" sideband of mode  $m$  with Rabi frequencies

$$\Omega_c = g_j J_\ell(k_x \xi_j) \prod_{k=1}^N \mathcal{R}_{j,k}(n_k) \quad (12a)$$

$$\Omega_{-1} = g_j J_\ell(k_x \xi_j) \prod_{\substack{k=1 \\ (k \neq m)}}^N \mathcal{R}_{j,k}(n_k) e^{-\eta_{j,m}^2/2} \eta_{j,m} \frac{L_{n_m-1}^1(\eta_{j,m}^2)}{\sqrt{n_m}} \simeq g_j J_\ell(k_x \xi_j) \eta_{j,m} \sqrt{n_m} \quad (12b)$$

$$\Omega_{+1} = g_j J_\ell(k_x \xi_j) \prod_{\substack{k=1 \\ (k \neq m)}}^N \mathcal{R}_{j,k}(n_k) e^{-\eta_{j,m}^2/2} \eta_{j,m} \frac{L_{n_m}^1(\eta_{j,m}^2)}{\sqrt{n_m+1}} \simeq g_j J_\ell(k_x \xi_j) \eta_{j,m} \sqrt{n_m+1}, \quad (12c)$$

where the approximations in Eqs. (12b) and (12c) hold in the Lamb-Dicke regime ( $\eta_{j,m} \sqrt{n_m} \ll 1$ ). The carrier transition, independent of  $n_m$ , simply rotates the internal level of ion  $j$  and can be used to initialize the quantum bit into the state  $(\alpha_j|\downarrow\rangle_j + \beta_j|\uparrow\rangle_j)$ , with  $\alpha_j$  and  $\beta_j$  arbitrary complex numbers satisfying  $|\alpha_j|^2 + |\beta_j|^2 = 1$ . The first red sideband interaction is the central ingredient of the Cirac-Zoller scheme. If motional mode  $m$  is initially prepared in the  $n_m = 0$  zero-point level, then by applying radiation to the  $j$ th ion on the first red sideband for a time  $\tau = \pi/2\Omega_{-1}$  (a  $\pi$  pulse), the state  $(\alpha_j|\downarrow\rangle_j + \beta_j|\uparrow\rangle_j)|0\rangle$  is mapped to  $|\downarrow\rangle_j(\alpha_j|0\rangle + \beta_j|1\rangle)$ ; that is, the quantum bit initially stored in the  $j$ th ion is mapped onto the first two states of motion of mode  $m$ . This information is shared among all ions which have nonzero  $\eta_{j,m}$  and can be subsequently mapped onto another ion  $j'$  to produce an arbitrary entangled state between ions  $j$  and  $j'$ . The operations of Eq. (12) have been realized on a single trapped  ${}^9\text{Be}^+$  ion [14,15].

## 2 Uniform Coupling

Here, we assume that each ion receives the same coupling from the radiation, or that each term in the sum of Eq. (7) is independent of  $i$ , outside of phase factors. This can occur when the applied radiation uniformly illuminates all of the trapped ions ( $g_i = g$ ). Furthermore, we require that (i)  $k_x \xi_i$  is independent of  $i$ , which holds in a linear trap ( $\xi_i = 0$ ) or in the case of copropagating Raman beams ( $k_x = 0$ ), and (ii) transitions are driven on the carrier or a uniform mode of motion  $u$  where the Lamb-Dicke parameter  $\eta_{i,u} = \eta_u$  is independent of  $i$  and the other (nonuniform) modes are in the Lamb-Dicke regime so that  $\mathcal{R}_{i,k} \simeq 1$ . Examples of uniform motional modes are the COM mode where  $\eta_{i,\text{com}} = \eta_{\text{com}} = k_x \sqrt{\hbar/2MN\omega_x}$  or the stretch mode for  $N = 2$  ions). For transitions on the carrier,

$$\mathcal{H}_{c_u}'' = \hbar g (J_+ + J_-), \quad (13)$$

and for transitions involving a uniform mode  $m_u$

$$\mathcal{H}_{1_u}'' = \hbar g \left( J_+ e^{i\eta_u(\hat{a}_u + \hat{a}_u^\dagger)} + h.c. \right). \quad (14)$$

In these expressions,  $J_\pm \equiv \sum_{i=1}^N S_\pm^i e^{\pm i\phi_i}$  are generalized angular momentum raising and lowering operators formed by combining the  $N$  spin- $1/2$  ions into an equivalent spin  $-J = N/2$  system [8]. If the system is

initially in the state  $|\downarrow\rangle_1|\downarrow\rangle_2\cdots|\downarrow\rangle_N = |J, m_J = -J\rangle$ , then evolution is confined to the  $2J + 1 = N + 1$  coupled eigenstates  $|J, m_J\rangle$  with matrix elements  $\langle J, m_J \pm 1 | J_{\pm} | J, m_J \rangle = \sqrt{J(J+1) - m_J(m_J \pm 1)}$ . (Unlike the usual angular momentum eigenstates, when these states are decomposed to the uncoupled states, there are generally different phase factors in front of each uncoupled state.) In these special cases of uniform couplings, evolution of the quantum state of the  $N$  ions is simplified because it is restricted to the subspaces spanned by the  $2m_J + 1 \leq N + 1$  states of the equivalent spin  $J = N/2$  system instead of the complete Hilbert space containing  $2^N$  states.

### 3 General Treatment of $N=2$ Ions

For the case of two ions, there are two axial modes of motion: the COM mode at  $\omega_{com} = \omega_x$  and the stretch (STR) mode where the ions move with opposite phase at  $\omega_{str} = \sqrt{3}\omega_x$ . The static fields at the two ion positions (balanced by the trapping fields) are  $F_{1,2} = \mp e/4\pi\epsilon_0 s^2 + F_{ext}$ , where  $s = \sqrt[3]{e^2/(2\pi\epsilon_0 m\omega_x^2)}$  is the spatial separation between the two ions. We can rewrite the general interaction of Eq. (7) for two ions:

$$\begin{aligned} \mathcal{H}_{2\text{ ions}}'' = & \hbar g_1 e^{i\ell\pi/2} J_{\ell}(k_x \xi_1) \left( S_+^1 e^{i\eta_{com}(\hat{a}_{com} + \hat{a}_{com}^\dagger) + i\eta_{str}(\hat{a}_{str} + \hat{a}_{str}^\dagger) - ik_x s/2} + h.c. \right) \\ & + \hbar g_2 e^{i\ell\pi/2} J_{\ell}(k_x \xi_2) \left( S_+^2 e^{i\eta_{com}(\hat{a}_{com} + \hat{a}_{com}^\dagger) - i\eta_{str}(\hat{a}_{str} + \hat{a}_{str}^\dagger) + ik_x s/2} + h.c. \right), \end{aligned} \quad (15)$$

where  $\eta_{com} = \eta_{1,com} = \eta_{2,com}$  and  $\eta_{str} = \eta_{1,str} = \eta_{2,str} = \eta_{com}/\sqrt[3]{3}$ .

## III QUANTUM LOGIC WITH A FEW IONS

### A Two Ions

At NIST, we have laser-cooled both axial modes of two  $^9\text{Be}^+$  ions to the ground state of motion in a trap with  $\omega_x/2\pi \simeq 10$  MHz [11]. The spacing between the ions is only  $s \simeq 2\mu\text{m}$  in such a strong trap, so it is not trivial to focus laser beams to individually address the two ions for quantum logic following Section II C 1. We therefore consider alternate schemes in which both ions are equally illuminated ( $g_1 = g_2$ ).

#### 1 Differential Addressing with Micromotion

It is still possible to differentially address the two ions by tuning the argument of the Bessel functions in Eq. (15) through the externally applied axial field  $F_{ext}$ . The micromotion amplitudes of the two ions are

$$\xi_{1,2} = \frac{e\alpha q}{2M\omega_x^2} \left( \mp \frac{e}{4\pi\epsilon_0 s^2} + F_{ext} \right), \quad (16)$$

so the corresponding carrier Rabi frequencies on the two ions can be set to any ratio  $\Omega_1/\Omega_2 = J_{\ell}(k_x \xi_1)/J_{\ell}(k_x \xi_2)$ . In Fig. 3(a), we have measured the Rabi frequencies of the two ions with  $\ell = 0$  while varying the externally applied field  $F_{ext}$ , showing excellent agreement with theory [12].

In particular, by setting  $F_{ext}$  so that  $\Omega_1/\Omega_2 = 2$  (vertical arrow in Fig. 3(a)) and initializing the ions in state  $|\downarrow\rangle|\downarrow\rangle|0_{str}\rangle$ , we can create the state  $|\downarrow\rangle|\uparrow\rangle|0_{str}\rangle$  by driving on the carrier for a time  $\tau = \pi/\Omega_1$  (vertical arrow in Fig. 3(b)). To make an EPR entangled state [25], we can then switch  $F_{ext}$  so that  $\Omega_1/\Omega_2 = 1 + \sqrt{2}$  and apply radiation tuned to  $\delta = -\omega_{str}$  and drive on the STR red-sideband which couples  $|\downarrow\rangle|\uparrow\rangle|0_{str}\rangle$ ,  $|\downarrow\rangle|\downarrow\rangle|1_{str}\rangle$ , and  $|\uparrow\rangle|\downarrow\rangle|0_{str}\rangle$ . This three-level system can be solved exactly, and we find that the state evolves to a maximally entangled EPR state

$$|\downarrow\rangle|\uparrow\rangle|0_{str}\rangle \longrightarrow \left( \frac{|\downarrow\rangle|\uparrow\rangle + e^{ik_x s} |\uparrow\rangle|\downarrow\rangle}{\sqrt{2}} \right) |0_{str}\rangle, \quad (17)$$

with the phase controlled by the spacing  $s$  of the two ions. In Ref. [12],  $F_{ext}$  was fixed for a 2:1 ratio of Rabi frequencies throughout the experiment, which created a similar but slightly less entangled version as Eq. (17).

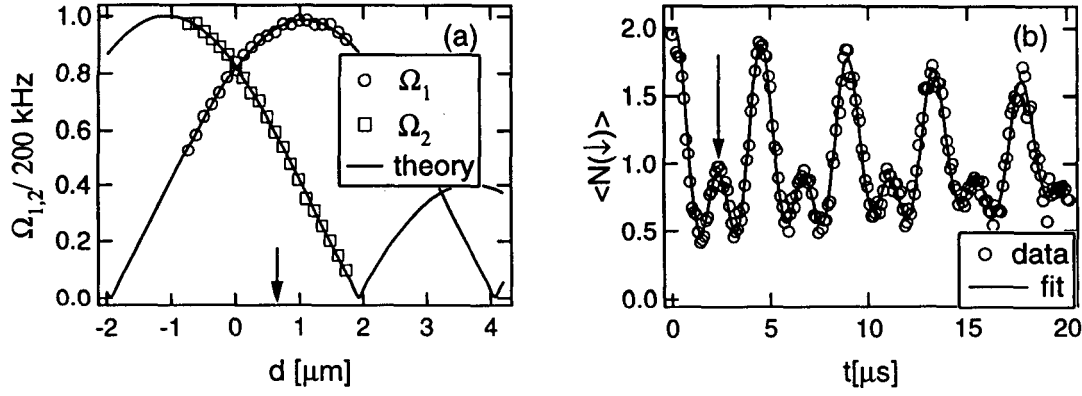


**FIGURE 3.** (a) Normalized carrier Rabi frequencies of each of two ions as a function of the mean position of the two ions  $d = (\bar{X}_1 + \bar{X}_2)/2 = eF_{ext}/m\omega_{com}^2$  set by externally applied uniform field  $F_{ext}$ . The solid curves are theoretical Bessel functions  $J_0(k_x\xi_1)$  and  $J_0(k_x\xi_2)$ , where  $\xi_i$  is from Eq. (16). (b) Number of ions in state  $|\downarrow\rangle$  as a function of the time the carrier is applied, clearly showing two frequency components with  $\Omega_1/\Omega_2 = 2$ . the arrow in (a) indicates the setting of  $d$  for (b).

This technique of tuning each ion's Rabi frequency based on unequal micromotion amplitudes can also be extended to give individual addressing of the ions as in Section II C 1 but without using focussed beams. Here, we set the trap strength and external electric field  $F_{ext}$  such that  $k_x\xi_1 = 0$  and  $k_x\xi_2 = 2.405$ . (In the NIST  ${}^9\text{Be}^+$  experiments where  $k_x = (k_2 - k_1) \cdot \hat{x} = \sqrt{2}(2\pi/\lambda_{Be})$  and  $\Omega_T/2\pi \simeq 240$  MHz, this condition is met when the axial COM frequency is set to  $\omega_x/2\pi \simeq 3.80$  MHz with  $U_0 \propto a = 0$  and the external field is set to  $F_{ext} = 1.01$  V/cm.) When ion 1 is to be isolated, the radiation is tuned so that  $\ell = 0$  in Eq. (6), thus shutting off the coupling to ion 2 since  $J_0(2.405) = 0$ . When ion 2 is to be isolated, the radiation is tuned so that  $|\ell| = 1$ , thus shutting off the coupling to ion 1 since  $J_1(0) = 0$ .

## 2 EPR State without Micromotion

We describe an alternate scheme for making EPR states where each ion is equally illuminated by the radiation and has the same coupling to the radiation field (in the case of a linear trap or for  $F_{ext} = 0$  in Eq. (16) giving  $|\xi_1| = |\xi_2|$ ). Here we can describe the system in terms of an equivalent angular momentum  $J = 1$  system described by quantum numbers  $|J, m_J\rangle$  and the stretch motional state  $|n_{str}\rangle$ . If the two ions are initialized in the state  $|\downarrow\rangle|\downarrow\rangle|0_{str}\rangle = |1, -1\rangle|0_{str}\rangle$ , then we find from Eqs. (11) and (14) that, if we tune to the first blue sideband of the stretch mode ( $\delta = \omega_{str}$ ), the couplings are

$$\langle 1, 0 | \langle 1_{str} | \mathcal{H}'' | 0_{str} \rangle | 1, -1 \rangle = \hbar g \mathcal{R}_{com}(n_{com}) e^{-\eta_{str}^2/2} \eta_{str} \sqrt{2} \quad (18a)$$

$$\langle 1, 1 | \langle 2_{str} | \mathcal{H}'' | 1_{str} \rangle | 1, 0 \rangle = \hbar g \mathcal{R}_{com}(n_{com}) e^{-\eta_{str}^2/2} \eta_{str} (2 - \eta_{str}^2), \quad (18b)$$

where  $\mathcal{R}_{com}(n_{com}) = \mathcal{R}_{1,com}(n_{com}) = \mathcal{R}_{2,com}(n_{com})$ . Now if the trap strength is set so that  $\eta_{str} = \sqrt{2}$ , the second coupling (Eq. (18b)) vanishes. The first coupling (Eq. (18a)) can then be driven for a time such that  $|1, -1\rangle|0_{str}\rangle$  evolves directly to the EPR entangled state  $|1, 0\rangle|1_{str}\rangle = (e^{i\phi_1} |\downarrow\rangle |\uparrow\rangle + e^{i\phi_2} |\uparrow\rangle |\downarrow\rangle) |1_{str}\rangle / \sqrt{2}$ .

## B Three Ions

For  $N = 3$  ions, we are interested in producing the maximally entangled ("GHZ") state [26]:

$$\Psi_{GHZ} = \frac{|\downarrow\rangle|\downarrow\rangle|\downarrow\rangle + e^{i\phi} |\uparrow\rangle|\uparrow\rangle|\uparrow\rangle}{\sqrt{2}}. \quad (19)$$

Such states are of great interest to the measurement of quantum nonlocality and can be employed for rudimentary quantum error correction codes [27]. This state can be produced using the general Cirac-Zoller scheme; here we discuss two schemes for generating (or approximating) Eq. (19) without individual addressing of ions.

## 1 Approximate GHZ State without Micromotion

We assume that the three ions are equally illuminated by the radiation fields ( $g_i = g$ ), undergo no micromotion, and are initialized in the state  $|\downarrow\rangle|\downarrow\rangle|\downarrow\rangle|0_{str}\rangle|0_{eg}\rangle$ . Here,  $|n_{str}\rangle$  refers to the stretch mode at frequency  $\sqrt{3}\omega_x$  wherein the middle ion is at rest, and  $|n_{eg}\rangle$  refers to the ‘‘Egyptian’’ [28] motional mode at frequency  $\omega_{eg} = \sqrt{29/5}\omega_x$  wherein the middle ion 2 moves out of phase and with twice the amplitude as the outer ions 1 and 3. We sequentially apply three pulses of radiation to the ions:

- (1) The radiation is tuned to the 2nd blue sideband of the Egyptian mode ( $n'_{eg} = n_{eg} + 2$  from Eq. (11)). This coupling, proportional to  $\eta_{i,eg}^2$ , is 4 times larger on the middle ion than on either outer ion. We therefore approximate that only the middle ion is affected. By applying this radiation for an approximate  $\pi/2$  pulse duration, we create a superposition of the original state with  $|\downarrow\rangle|\uparrow\rangle|\downarrow\rangle|0_{str}\rangle|2_{eg}\rangle$ .
- (2) The motion in the Egyptian mode is swapped with the motion in the stretch mode. This can be accomplished by tuning the radiation so that  $\omega_L = \omega_{eg} - \omega_{str}$ . In this case, a different rotating-wave approximation is performed in Section II C, and Eq. (3) is reproduced *without the internal  $S_{\pm}^i$  operators*. The three motional states  $|0_{str}\rangle|2_{eg}\rangle$ ,  $|1_{str}\rangle|1_{eg}\rangle$ , and  $|2_{str}\rangle|0_{eg}\rangle$  are coupled without affecting the internal states of the ions, allowing  $|0_{str}\rangle|2_{eg}\rangle$  to evolve to  $|2_{str}\rangle|0_{eg}\rangle$  through the intermediate  $|1_{str}\rangle|1_{eg}\rangle$  state for  $\eta_{i,str}, \eta_{i,eq} \ll 1$ .
- (3) The radiation is tuned to the first red sideband of the stretch mode. This operation does not affect the middle ion ( $\eta_{2,str} = 0$ ) and largely removes the two quanta in the stretch mode while simultaneously flipping the outer two internal states. The three steps roughly give the evolution (ignoring phase factors):

$$|\downarrow\rangle|\downarrow\rangle|\downarrow\rangle|0_{str}\rangle|0_{eg}\rangle \longrightarrow \frac{|\downarrow\rangle|\downarrow\rangle|\downarrow\rangle|0_{str}\rangle|0_{eg}\rangle + |\downarrow\rangle|\uparrow\rangle|\downarrow\rangle|0_{str}\rangle|2_{eg}\rangle}{\sqrt{2}} \quad (20a)$$

$$\longrightarrow \frac{|\downarrow\rangle|\downarrow\rangle|\downarrow\rangle|0_{str}\rangle|0_{eg}\rangle + |\downarrow\rangle|\uparrow\rangle|\downarrow\rangle|2_{str}\rangle|0_{eg}\rangle}{\sqrt{2}} \quad (20b)$$

$$\longrightarrow \frac{|\downarrow\rangle|\downarrow\rangle|\downarrow\rangle|0_{str}\rangle|0_{eg}\rangle + |\uparrow\rangle|\uparrow\rangle|\uparrow\rangle|0_{str}\rangle|0_{eg}\rangle}{\sqrt{2}} \quad (20c)$$

The actual amplitudes of the states must be solved numerically due to imperfections in the first and third steps. As a consequence, instead of a perfect GHZ state, this scheme generates the state  $|\Psi_{MIKKLMTWW}\rangle$  with a fidelity  $|\langle\Psi_{MIKKLMTWW}|\Psi_{GHZ}\rangle|^2 \simeq 86\%$ .

## 2 Exact GHZ State with Micromotion

Here, the ions are again equally illuminated, but the three ions have different couplings to the radiation due to different amounts of micromotion in each ion. In particular, we set axial trap strength and external field such that  $k_x\xi_{1,3} = 2.405$  and  $k_x\xi_2 = 0$ . This allows the middle ion 2 to be individually addressed for  $\ell = 0$  (since  $J_0(2.405) = 0$ ), and outer ions 1 and 3 to be equally addressed for  $\ell = 1$  (since  $J_1(0) = 0$ ). (In the NIST  $^9\text{Be}^+$  experiments, following the parameters of section III A 1, this condition is met when the axial COM frequency is set to  $\omega_x/2\pi \simeq 6.08$  MHz with  $U_0 \propto a = 0$  and the external field is set to  $F_{ext} = 0$ .) We sequentially apply two pulses of radiation to the ions, initially prepared in the state  $|\downarrow\rangle|\downarrow\rangle|\downarrow\rangle|0_m\rangle$ :

- (1) A  $\pi/2$ -pulse is driven on the first blue sideband of motional mode  $m$  with  $\ell = 0$ , affecting only the middle ion:

$$|\downarrow\rangle|\downarrow\rangle|\downarrow\rangle|0_m\rangle \longrightarrow \frac{|\downarrow\rangle|\downarrow\rangle|\downarrow\rangle|0_m\rangle + e^{i\phi_2}|\downarrow\rangle|\uparrow\rangle|\downarrow\rangle|2_m\rangle}{\sqrt{2}} \quad (21)$$

- (2) A pulse is driven on the first red sideband of mode  $m$  with  $\ell = 1$ , affecting the outer two ions identically. If we set the Lamb-Dicke parameter to  $\eta_{m,1} = \eta_{m,3} = \sqrt{2} - \sqrt{2}$ , we find that the two-ion couplings similar to Eq. (18) are identical, and after a particular time the state evolves to the GHZ state

$$\frac{|\downarrow\rangle|\downarrow\rangle|\downarrow\rangle|0_m\rangle + e^{i\phi_2}|\downarrow\rangle|\uparrow\rangle|\downarrow\rangle|2_m\rangle}{\sqrt{2}} \longrightarrow \frac{|\downarrow\rangle|\downarrow\rangle|\downarrow\rangle|0_m\rangle + ie^{i(\phi_1+\phi_2+\phi_3)}|\uparrow\rangle|\uparrow\rangle|\uparrow\rangle|0_m\rangle}{\sqrt{2}} \quad (22)$$

Since all axial trap frequencies (proportional to  $\omega_x$ ) are constrained by the micromotion requirements above, one of the nonaxial modes must be used for mode  $m$ . Since the Lamb-Dicke parameter is large, this mode

should be very weakly bound. For three ions, there are two “zig-zag” modes in which all three ions move along  $y$  or  $z$ , with the middle ion 180 degrees out of phase with the outer two ions. The oscillation frequency of the  $z$  zig-zag mode is  $\omega_{zzz} = \sqrt{\omega_z^2 - 2.4\omega_x^2}$ , which can be made arbitrarily small while keeping all 8 other modes at relatively high frequencies. For our NIST  ${}^9\text{Be}^+$  experiments, we find that  $\eta_{1,zzz} = \eta_{3,zzz} = \sqrt{2 - \sqrt{2}}$  implies a zig-zag frequency of  $\omega_{zzz}/2\pi \simeq 64$  kHz.

## IV OUTLOOK

A scalable scheme for universal quantum logic with trapped ions is the method Cirac and Zoller proposed in which the individual ions in a string are individually addressed with laser radiation (Section II C 1). However, there are many degrees of freedom of up to 3 ions which can allow quantum logic gates and entangled states to be created without individual addressing. Although these schemes do not appear scalable within a single collection of ions, they may prove useful for doing quantum logic on nodes of a few ions which could then be coupled to other nodes of ions with cavity-QED techniques [29,30] or ion accumulators in which an individual ion is physically moved to a nearby separate collection of ions [22].

Work of the U.S. government; not subject to copyright. We gratefully acknowledge support from the National Security Agency, Office of Naval Research, and Army Research Office. We thank Matt Young for critical comments regarding the manuscript.

## REFERENCES

1. D. P. DiVincenzo, *Science* **270**, 255 (1995).
2. A. Ekert and R. Jozsa, *Rev. Mod. Phys.* **68**, 733 (1996).
3. D. Deutsch, *Proc. Roy. Soc. London A* **425**, 73 (1989).
4. P. W. Shor, *SIAM J. Comp.* **26**, 1484 (1997).
5. L. K. Grover, *Phys. Rev. Lett.* **79**, 325 (1997).
6. S. Lloyd, *Science* **261**, 1569 (1993).
7. *Quantum Theory and Measurement*, edited by J. A. Wheeler and W. H. Zurek (Princeton University Press, Princeton, N.J., 1983).
8. D. J. Wineland, J. J. Bollinger, W. M. Itano, and D. J. Heinzen, *Phys. Rev. A* **50**, 67 (1994).
9. J. J. Bollinger, W. M. Itano, D. J. Wineland, and D. J. Heinzen, *Phys. Rev. A* **54**, R4649 (1996).
10. J. I. Cirac and P. Zoller, *Phys. Rev. Lett.* **74**, 4091 (1995).
11. B. E. King *et al.*, *Phys. Rev. Lett.* **81**, 1525 (1998).
12. Q. A. Turchette *et al.*, LANL e-print archive quant-ph/9806012 (1998).
13. J. J. Bollinger *et al.*, *IEEE Trans. Instr. Meas.* **40**, 126 (1991).
14. C. Monroe *et al.*, *Phys. Rev. Lett.* **75**, 4011 (1995).
15. C. Monroe *et al.*, *Phys. Rev. Lett.* **75**, 4714 (1995).
16. R. Blatt and P. Zoller, *Eur. J. Phys.* **9**, 250 (1988).
17. H. G. Dehmelt, *Adv. Atom. Mol. Phys.* **3**, 53 (1967).
18. M. G. Raizen *et al.*, *J. Mod. Opt.* **39**, 233 (1992).
19. J. P. Schiffer, *Phys. Rev. Lett.* **70**, 818 (1993).
20. A. Steane, *Appl. Phys. B* **64**, 623 (1997).
21. D. James, *Appl. Phys. B* **66**, 181 (1997).
22. D. J. Wineland *et al.*, *J. Res. Nat. Inst. Stand. Tech.* **103**, 259 (1998).
23. G. Schrade *et al.*, *Appl. Phys. B* **64**, 181 (1997).
24. H. J. Lipkin, *Quantum Mechanics* (North-Holland, New York, 1973).
25. A. Einstein, B. Podolsky, and N. Rosen, *Phys. Rev.* **47**, 777 (1935).
26. D. M. Greenberger, M. A. Horne, Shimony, and A. Zeilinger, *Am. J. Phys.* **58**, 1131 (1990).
27. P. W. Shor, *Phys. Rev. A* **52**, R2493 (1995).
28. W. H. Zurek, private communication.
29. J. I. Cirac, P. Zoller, H. J. Kimble, and H. Mabuchi, *Phys. Rev. Lett.* **78**, 3221 (1997).
30. T. Pellizzari, *Phys. Rev. Lett.* **79**, 5242 (1997).